Proceedings Australian Geothermal Energy Conferences 2013
Brisbane, Australia, 14-15 November 2013

Diagenesis Impact on the Reservoir Quality of the Hutton Sandstone, Cooper Basin, South Australia

Antoine Dillinger, Cameron Huddlestone-Holmes, Ludovic P. Ricard, Lionel Esteban and Horst Zwingmann

CSIRO Earth Science and Resource Engineering, 26 Dick Perry Avenue, Kensington WA 6151

antoine.dillinger@csiro.au

Keywords: Diagenesis, porosity, permeability, reservoir quality, geothermal, Hutton Sandstone, Cooper Basin, Eromanga Basin

ABSTRACT

The Hutton Sandstone (Cooper-Eromanga Basin, SA) recently became a target for geothermal heat extraction due to its potential for high natural permeability, decent temperatures, and high reservoir volume. However, recent exploratory drilling conducted by Origin Energy Ltd and Geodynamics Ltd at the Celsius-1 well didn't produce the anticipated flow rates, raising the question of the impact of the diagenesis on the reservoir quality of this sedimentary formation.

Previous studies focused on oil and gas fields located on the ridges of the Nappamerri Trough highlighted the good reservoir quality of the upper Hutton Sandstone. Nevertheless, an extensive literature review reveals that the middle part of the Nappamerri Trough – where Celsius-1 is situated – remains poorly investigated. This study aims to better characterize the petrophysical and petrological properties as well as the diagenesis processes occurring within the Hutton Sandstone. It is based on drill cuttings and cores retrieved from Celsius-1 and other existing nearby stratigraphic and petroleum exploration wells (Della-2, Merrimelia-19, Strzelecki-17 and Packsaddle-1).

Porosity and pore size distribution of the Celsius-1 drill cuttings were first measured by using a laboratory low field Nuclear Magnetic Resonance (NMR) under water-saturated condition. Permeability was then inferred from NMR transversal relaxation time T2 via the empirical equation of Timur-Coates. The petrology of the Hutton Sandstone was studied via three different analytical tools: i) Basic automated QEMSCAN for phase assemblage mapping and quantitative analysis of the mineralogy; ii) Scanning Electron Microscope for visualizing the pore geometry and secondary mineral growths; iii) Optical Microscopy for high precision characterization of the mineralogy, the micro-structures, the pore connectivity and the diagenetic cements.

The integration of these results gives a robust and complementary evaluation of the diagenetic history in a deep burial environment, its effects on the flow properties of the Hutton Sandstone, and its regional extent.

1. INTRODUCTION

Geothermal resources hosted within sedimentary basins, also known as Hot Sedimentary Aquifers (HSA), have been successfully explored and developed for geothermal energy extraction worldwide (Lund et al., 1998, 2011). The best known examples in Australia are in Birdsville, the Latrobe Valley hot-springs and several projects in Perth (Pujol, 2011). These areas have been targeted because of their potential high natural permeability, the presence of water, suitable temperatures and the extent of the resources. Similarly, the Hutton Sandstone – a deep HSA resource – has been tested via deep exploratory drilling at the Celsius 1 well in the Cooper-Eromanga Basin (South Australia). This resource was targeted as it was thought to have high natural matrix permeability similar to the prolific adjacent oil and gas fields, and was not expected to require significant permeability enhancement. Moreover, the region around Celsius 1 is known to be underlain by radiogenic granites, providing heat to the overlying formations including the Hutton Sandstone. Celsius 1 was drilled to intersect the full thickness of the Hutton Sandstone section and evaluate the flow capacity of the formation to investigate the exploitation potential of this known heat resource. However, well tests did not produce the anticipated flow rates at the resource temperatures required to generate electricity, raising the question of the impact of the diagenesis on the reservoir quality of the sedimentary formation.

The objectives of the study proposed herein are (i) to give a better insight of the Hutton Sandstone by compiling, classifying and analysing the well bore data provided by existing adjacent stratigraphic or petroleum exploration wells; (ii) to provide information on the diagenetic processes and history affecting the flow properties of the target formation by the analysis of drill cuttings retrieved from Celsius 1 and other offset wells, including mineralogy mapping by Qemscan and imaging by Scanning Electron Microscope and optical microscopy; (iii) to acquire new data on the evolution of petrophysical properties, especially the permeability, of the Hutton Sandstone by the use of a Nuclear Magnetic Resonance on the drill cuttings along with Logging While Drilling (LWD) logs.

The integration of all these results provides a strong geological characterization of the Hutton Sandstone. The outcomes give a robust evaluation of the diagenetic history in a deep burial environment, its effects on the flow properties of the Hutton Sandstone, and implications for the geothermal potential of siliciclastic formations.

2. GEOLOGICAL BACKGROUND

The Cooper Basin consists of a broad downwarp with two main depocentres – the Poolowanna Trough and the Cooper region – separated by the north-east-trending Birdsville Track Ridge, a complex of related domes and ridges. Three major troughs in the Cooper region (Patchawarra, Nappamerri and Tenappera) are separated by structurally high ridges (GMI and Murteree Ridges)

associated with the reactivation of northwest-directed thrust faults in the underlying Warburton Basin (Fig. 1). The Nappamerri Trough contains the deepest and thickest Cooper Basin sediments. Deposition in the Jurassic to Cretaceous Eromanga Basin was initially controlled by the topography of the Triassic Nappamerri unconformity surface, especially for the Poolowanna Formation and lower Hutton Sandstone. No major depositional breaks occur in the Eromanga Basin, indicating a period of tectonic quiescence. Mesozoic deformation was thus relatively weak and consisted of regional tilt, drape and compaction with progressive burial (Gravestock 1998). The Tertiary east-west compression enhanced reactivation and closure of pre-existing structural patterns (Kuang 1985). Geothermal gradients, already high due to subcrop of uraniferous granite on the floor of the Nappamerri Trough, have been elevated still further in the past 2-5 million years.

The region forms part of a broad area of anomalously high heat flow, which is attributed to Proterozoic basement enriched in radiogenic elements. High heat producing granites, including granodiorite of the Big Lake Suite (BLS) at the base of the Copper/Eromanga sequences, form a significant geothermal play that was targeted to be Australia's first Hot Rock development at Habanero. The relationship between high heat flow, high temperature gradient and anomalous heat production in the BLS is well established. The thick sedimentary sequences of the overlying Cooper/Eromanga Basins provide a thermal blanketing effect resulting in temperatures as high as 270 °C at depths < 5 km.

The Lower to Middle Jurassic Hutton Sandstone consists of mineralogically mature, fine to coarse grained quartzoses with minor siltstone interbeds. The formation contains sands sourced from a cratonic provenance and clasts reworked from Triassic, Permian and older sediments. The Hutton Sandstone was deposited in braided stream to high energy, low sinuosity fluvial environments with influence from aoelian and lacustrine processes (Watts 1987). The wells drilled to date in the Eromanga Basin have been on structural plays and approximately 70 % of the oil discovered is reservoired in the Hutton Sandstone and sealed by the Birkhead Formation.

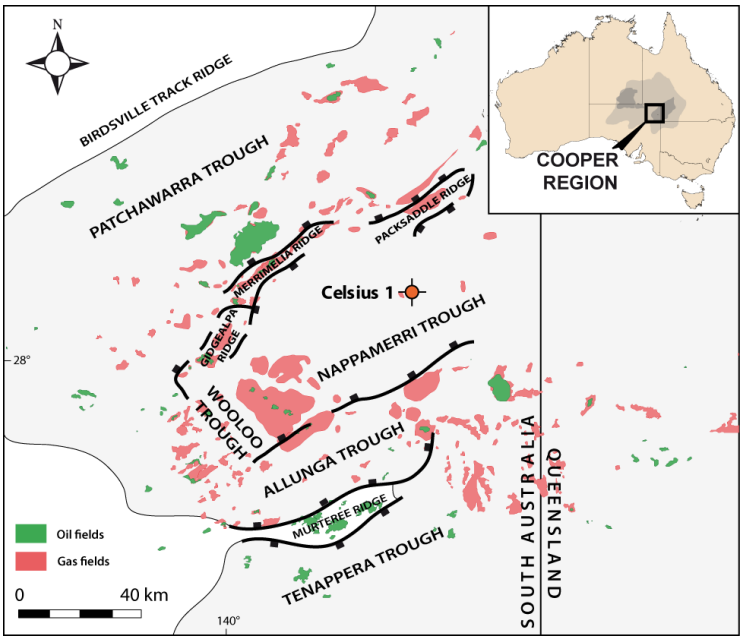

Figure 1: Structural map of the Cooper region and Oil & Gas fields

3. PETROLOGY OF THE HUTTON SANDSTONE

3.1 Celsius 1

3.1.1 Qemscan analysis

Variations in mineralogy across the Hutton Sandstone are best explained by a lithofacies control rather than systematic variations with depth. This aspect leads to define a lithofacies classification scheme based on the mineral area percentage provided by Qemscan analysis. Therefore, five lithofacies have been identified among the Celsius 1 cuttings.

Lithofacies A is the most common facies within the sample set. Its main features are a high abundance of quartz (> 90 %) and low amounts of feldspar (< 1 %), micas/illite (< 3 %), kaolinite (< 1 %), and other mineral phases (< 2 %). High quartz/(quartz + feldspars) ratio (> 90 %) and low percentages of matrix (< 4 %) lead to a classification of this sandstone as a quartz arenite. **Lithofacies B** is also quartz-dominated (70 – 90 %) although it exhibits slightly higher amounts of micas/illite (4 – 9 %) and other mineral phases (2 – 12 %) than facies A. This sandstone is classified as a quartz wacke due to quartz/(quartz + feldspars) ratio over 95 % and percentages of matrix higher than 6 %. Facies B is divided into two sub-facies B1 and B2. **Sub-facies B1** shows numerous disconnected mica/clay aggregates heterogeneously distributed in the quartz matrix. No bedding is observed. **Sub-facies B2** differs from sub-facies B1 by its relatively higher content in kaolinite (< 1.5 % for B1; between 2.5 and 6.5 % for B2) observed as large kaolinite aggregates on the Qemscan images. **Lithofacies C** presents low percentages of quartz (40 – 70 %), significant amounts of micas/illite (up to 30 %) and intermediate amounts of feldspar and kaolinite (2 – 5 %). High quartz/(quartz + feldspars) ratio (> 90 %) and intermediate percentages of matrix (between 22 and 45 %) lead to a classification of this sandstone as a quartz wacke as well. However, this facies differs from the previous ones by the interconnectivity of the micas/illites forming occasionally large clay aggregates or laminations. **Lithofacies D** is classified as a mudstone with high amounts of matrix (> 35 %) and low

quartz/(quartz + feldspars) ratio (< 45 %) and is interpreted as being contaminated by the water-based drilling mud used to remove cuttings from the borehole (KCl/Polymer in the case of Celsius 1).

Quantitative reports are provided by Qemscan for each scan where the percentages of each mineral phase (and pores) detected are derived from the specific area covered by the mineral. A reasonable trend can be noted when the facies distribution is plotted as a function of depth: facies A tends to be more represented towards the top of the formation while micas/clay-bearing sandstones (facies B1, B2 and C) appears more frequent towards the base. This characteristic can be explained by the migration and evolution of the depositional systems over time generating variable sediment compositions.

3.1.2 Imaging of the Celsius 1 drill cuttings by Scanning Electron Microscope

With no surprise, the mineral framework of all facies (except facies D) is mainly constituted of sub-angular detrital quartz grains, with sizes form medium silts to very coarse sands (10 to 1000 µm). The grain contacts essentially consist of line or suture contacts due to moderate to high mechanical compaction. Depending on the facies, grains are cemented and tightly interlocked by a fine-grained clayey matrix or a secondary cement, implying variable pore geometries and distributions. The dispersed argillaceous matrix exhibits characteristics of detrital clays with tiny, ragged abraded platelets (10 to 200 µm) naturally filling pores, coating the framework grains and creating pore-lining and pore-bridging fabrics. Unlike allogenic clays, authigenic cements develop within the sand subsequent to burial and thus are recognized by their delicate morphology which precludes sedimentary transport (Wilson & Pittman, 1977). Diagenetic cements occur here as sharp edged quartz overgrowths precipitated in optical continuity around the detrital quartz grains or pore-filling aggregates in interstitial or vugular pores with no apparent alignment to the framework grains. The most ubiquitous and widespread authigenic phases are quartz overgrowths and neoformation of kaolinite regardless of the facies. Neoformation of illite derived from the detrital matrix is the third most common authigenic process observed within the cuttings, with a frequency increasing with depth as the facies become increasingly clay-rich. This seems to be the main mode of formation of illite while kaolinite recrystallisation into illite is less widespread, perhaps due to the relative stability of kaolinite.

The correlation of all these observations enables the reconstruction of the diagenetic history of the studied interval. Sandstones of the Hutton Sandstone are affected by diagenetic processes of the eogenetic and mesogenetic phases. Nevertheless, the diagenesis affects the sediment in various fashions according to its initial composition. The facies classification scheme helps highlight three different diagenetic histories of the sandstone (Fig. 2).

Facies A shows processes of early diagenesis and hence has undergone a diagenetic evolution less pronounced than the other facies. Line grain contacts and brittle deformation of micas indicate moderate mechanical compaction and beginning of pressure solution. Its primary arenite composition depleted in clay matrix favors the development of silica cements while kaolinite and illite authigenesis are of less importance. No mesogenetic reaction has been recorded. **Facies B** exhibits features of advanced eogenesis and early mesogenesis with both line and sutured grain contact and ductile deformation of micas pointing to moderate to high compaction of the sediment. Its medium to high content in clay matrix and ferromagnesians leads to the formation of argillaceous cements such as kaolinite or illite and chlorite derived from micas. Sub-facies B1 differs from B2 by its abundance of illite replacing the clayey matrix or primary kaolinite. Sub-facies B2 is characterized by its kaolinite-rich composition originated from the clayey matrix or feldspars. Facies B also shows an example of authigenic muscovite as an evidence of early mesogenesis. The processes seen in **facies C** highlight the advanced stages of diagenesis affecting the formation. Numerous sutured grain contacts and widespread authigenic quartz and clays confirm the late eogenetic stage undergone by the sandstone. Moreover, occurrences of kaolinite-derived chlorite, authigenic mica and titaniferous minerals are strong evidences for an advanced stage of mesogenesis.

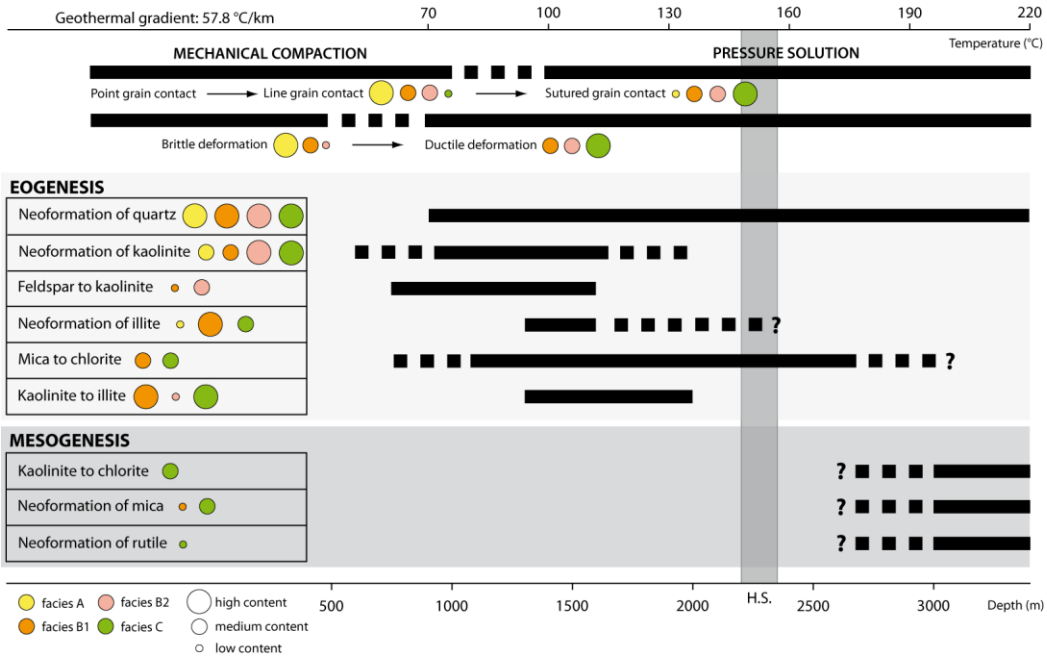

Figure 2: Timing of the burial diagenesis. Occurrence and relative frequency of the diagenetic processes in each facies are represented by colored circles. H.S. locates the Hutton Sandstone at Celsius 1

3.2 Offset wells

Samples of the Hutton Sandstone were retrieved from seven different wells located in the vicinity of Celsius. 1. In a general way, the textural and diagenetic characteristics of the Hutton Sandstone at different locations of the basin are comparable to the ones listed at Celsius 1. Textures of the grain frameworks highlight low to high mechanical compaction, brittle to ductile deformation and pressure solution depending on the position in the basin. The diagenetic cements are mainly composed of quartz overgrowths or kaolinite booklets derived from the alteration of feldspars of recrystallisation of the detrital clayey matrix. The absence of sericite in the Celsius 1 cuttings contrary to the other samples of the Nappamerri Trough can be explained by the difficulty to observe sericite minerals via SEM. Minor features with negligible impact on porosity such as muscovite or chlorite neoformation also appear. However, the chief difference between the offset well samples and Celsius 1 reside in the occurrence of calcite and widespread iron oxide cementation. It is worth noticing that the quartz-rich sandstones studied in offset wells mostly belong to facies A of the facies classification scheme. Unlike Celsius 1, facies B and C are trivial or absent in the samples from offset wells, possibly due to the available cores predominantly being from the oil bearing horizons at the top of the Hutton Sandstone.

4. PETROPHYSICAL PROPERTIES OF THE HUTTON SANDSTONE

4.1 Available porosity-permeability data

A significant amount of petrophysical analyses is available for the Hutton Sandstone. Combined porosity-permeability analyses on cores have been performed under ambient conditions for over 449 samples in 22 wells. Porosities plotted against permeabilities clearly show that the porosity of the Hutton Sandstone ranges mainly between 12 and 25 % while the permeability span is from 100 mD to 5000 mD with a low stress sensitivity (ambient permeability). High permeabilities combined with low stress sensitivities suggest a stiff formation behaviour that is usually related to tightly cemented sandstones.

The NNE Acrasia 1 (76 km away from Celsius 1) and WSW Tantanna 3 (105 km away from Celsius 1) petroleum wells possess numerous core analyses helpful for formation evaluation. Data from individual fields (Gidgealpa, Merrimelia or Strzelecki) have been grouped to improve the relevancy of the statistical distributions assuming the same deposition and diagenetic framework within a field. Median porosity values under ambient conditions range from 16.2 % (Acrasia 1) to 20.9 % (Gidgealpa field), the Merrimelia field and Tantanna 3 well also having values above 20 %. Apart from Tantanna 3, the variability can be considered as low (less than 5 % porosity difference between the 25^{th} percentile and the 75^{th} percentile). The three fields close to Celsius 1 exhibit high median permeability values under ambient conditions, from 748 mD for the Gidgealpa field to 1069 mD for the Merrimelia field, and high permeability ranges (from 326 to 1861 mD between the 25^{th} percentile and the 75^{th} percentile). Core analyses performed in the Gidgealpa field however yield a higher variability for the permeability with some very low values compared to the other wells and fields. The proximity of the Gidgealpa Ridge could be of very important for the circulation and composition of the diagenetic fluids. The far away Tantanna 3 well produces the lowest median permeability (50 mD) and permeability range (from 9 to 944 mD between the 25^{th} percentile and the 75^{th} percentile).

4.2 Nuclear Magnetic Resonance on the Celsius 1 drill cuttings

The NMR T_2 transversal relaxation time distribution provides significant information on the pore structure and the interactions between the pore fluids and pore surfaces. A T_2 distribution often displays a bi-modal behavior with (i) a short component (T_2s), proving the existence of micro-pores filled with irreducible capillary bound water or clay bound water; (ii) a long component (T_2l) corresponding to the inter-grain macro-porosity. The high variability of facies encountered in the sample set tends to produce noticeable changes in terms of porosity distribution and contribution of T_2s and T_2l due to different texture and clay content, leading to variable positions of the peaks (i.e. the contribution of the specific pore size populations). Three distinct behaviors of the NMR signal can be distinguished: (i) a strong contribution of T_2s (< 6 ms) and a weak T_2l related to high clay content and cements filled with clay bound water, and sparse macro-porosity; (ii) a well-developed T_2l centered around 40 ms and negligible T_2s contribution associated to large pores where the water is free to flow in a clean grain framework; (iii) an uni-modal distribution with only one peak centred around 7 ms related to clay inter-layer filled with capillary bound water.

The middle part of the Hutton Sandstone (2232 – 2283 m) exhibits a well-expressed T_2l component where water sits in large pores and is free to flow which suggests encouraging permeability values. The weak T_2s component reflects the low amounts of clays and cements in this section. The effective porosity should be close to the total porosity. This interval corresponds to two sets of decent porosity seen on the Compensated Neutron porosity Corrected log (CNC). The NMR analysis also confirms the poor porosity and flow capacity of the top part of the formation (above 2230 m) previously observed on the CNC log. Well-developed T_2s indicate that water resides in tiny pores sitting between clay layers (intergranular porosity). This feature reflects the advanced diagenesis affecting this section which led to the neoformation of siliceous and argillaceous cements acting as barrier to fluid flow. Similarly, the lower part of the Hutton Sandstone clearly shows uni-modal distributions of T_2 associated to capillary bound water trapped in pore throats.

Porosity data derived from NMR measurements show strong discrepancies with the CNC porosity log in the supposed “shaly” parts of the interval (top, base and medium break) where low CNC values are associated with high NMR porosities (up to 37 %). This peculiarity can be explained by the interaction between water and clays (abundant in these intervals) during laboratory saturation generating micro-cracks in turn artificially increasing the porosity. However, the middle part with decent porosity exhibits encouraging correlations between CNC log and NMR data. Average NMR porosities calculated in the section 2230 – 2303 m are 14.5 % from first amplitude and 15.1 % after inversion. Inferred values for permeability have been deduced from NMR porosities after inversion in this interval following the equation of Coates (Timur, 1968; Coeates et al., 1991; Coates et al., 1998). The average permeability within this restricted section of the Hutton Sandstone is 6.26 mD, with a minimum value of 0.0189 mD at 2301 m MDRT and a maximum value of 36.5 mD at 2232 m MDRT.

6. DISCUSSION

The study of the available core analysis in the Cooper Basin demonstrates the good reservoir quality of the Hutton Sandstone, in particular for the Merrimelia and Strzelecki fields both lining the Nappamerri Trough. The continuity of the petrophysical properties over a wide area is however not obvious, especially when considering local variations as observed in the Gidgealpa field. Nevertheless it gives a first broad insight of the porosity and permeability values that can be expected for Celsius 1.

The unexpected low flow rates recorded at Celsius 1 compared with the good reservoir quality of the adjacent fields is likely to be due to the preservation of a broad detrital clayey matrix and the extensive occurrence of authigenic filamentous illite, especially in facies B1 and C at the top and base of the Hutton Sandstone, and silica cements in facies A. These two types of clay minerals have been proven to severely occlude the pore space and reduce the permeability. The overall amounts of illitic material detected by Qemscan quantitative analysis confirm this assumption: 6.2 % at Celsius 1 (max: 30.7 %), 1.4 % at Packsaddle 1 (max: 2.9 %), and 1.0 % at Strzelecki 17 (max: 5.1 %).

This characteristic is confirmed by NMR T_2 transversal relaxation time distribution becoming shorter beyond 2295 m, when facies B1 and C are more common. The unimodal distribution observed in this interval is due to the peculiar texture of the sandstone that has maintained porosity while the diagenetic processes have impacted its permeability. This notably happens when filamentous pore-lining and pore-bridging authigenic illite develop within the poor space and severely reduces the permeability without affecting the porosity. This aspect has been widely observed by Scanning Electron Microscope at similar depths in the Celsius 1 sample set.

Sandstones of the Hutton Sandstone are affected by diagenetic processes of the eogenetic and mesogenetic phases. However, the Hutton Sandstone at Celsius 1 (2211 – 2355 m) is presently at pressure-temperature conditions that are below the mesogenetic conditions required to engage the processes observed in facies C (beyond 3000 m burial)., This suggests a late uplift and cooling from maximum palaeotemperatures. This interpreted history is corroborated by the occurrence of iron oxide cements in the offset wells postdating all the other authigenic minerals and also implies an uplift of the formation into the meteoric ground water zone. This particular feature was first discussed in Geotrack (1999) and later confirmed by Zwingmann et al. (2001).

The results of this study indicate that the negligible flow rates obtained from Celsius-1 was due to low permeabilities within the Hutton Sandstone. These low permeabilities are the results of diagentic processes.

REFERENCES

Coates, G.R., Miller, M., and Henderson, G., 1991. An investigation of a new magnetic resonance imaging log. Paper DD, in 32nd Annual Logging Symposium transactions: Society of Professional Well Log Analysts

Coates, G.R., Marschall, D., Mardon, D., and Galford, J., 1998. A new characterization of the bulk volume irreducible using magnetic resonance. *The Log Analyst*, Vol. 39, n°1 (January-February 1998), 51-63

Geotrack, 1999. Thermal history reconstructions in the Cooper-Eromanga Basin using zircon and apatite fission track analysis, and vitrinite reflectance with results from Beanbush-1, Burley-1, Burley-2, Dullingari-1, McLeod-1, Tirrawarra-1 and Toolachee wells (Report commissioned by PIRSA) Geotrack International Report 668, 103Gravestock, D.I., Hibburt, J.E., Drexel, J.F. (Eds), 1998. The petroleum geology of South Australia. Vol. 4: Cooper Basin. South Australia, Department of Primary Industries and Resources

Kuang, K.S., 1985. History and style of Cooper-Eromanga Basin structure. *Exploration Geophysics* (Melbourne), 16(2-3), 245-248

Lund, J.W., Freeston, D.H., and Boyd, T.l., 2011. Direct utilization of geothermal energy 2010 worldwide review. *Geothermics*, 40, 159-180

Lund, J.W., Lienau, P.J., and Lunis, B.C., 1988. Geothermal direct-use engineering and design guidebook. Third edition: Geo-Heat Centre, Oregon Institute of Technology

Pujol, M., 2011. Examples of successful hot Sedimentary Aquifer direct-use projects in Perth, Western Australia. In: Middleton, M. & Gessner, K. (eds). Western Australian Geothermal Energy Symposium. Perth, Western Australia, 23

Timur, A., 1968. An investigation of permeability, porosity, and residual water saturation relationships for sandstone reservoirs. The Log Analyst, 9, 8-17

Watts, K.J., 1987. The Hutton Sandstone – Birkhead Formation transition, ATp 269P(1), Eromanga Basin. *The APEA Journal*, 27, 215-229

Wilson, M.D., and Pittman, E.D., 1977. Authigenic clays in sandstones: Recognition and influence on reservoir properties and Paleoenvironmental analysis. *Journal of Sedimentology and Petrology*, 47, n°1 (March 1977), 3-31

Zwingmann, H., Tingate, P.R., Lemon, N.M., and Hamilton, P.J., 2001. K-Ar dating, petrographic and thermal modelling constraints on illite origin in the Cooper Basin, South Australia. *PESA Eastern Australasian Basins Symposium*, Melbourne, 321-327